Correction of Cupping Artifacts in Mega Volt Cone Beam CT Images

Steven F. Petit , Wouter J.C. van Elmpt, Sebastiaan M.J.J.G. Nijsten, André L.A.J. Dekker and Philippe Lambin
Department of Radiation Oncology (Maastro), GROW, University Hospital Maastricht, Maastricht the Netherlands

Introduction

For accurate three dimensional (3D) dose reconstruction the patient must be imaged during or just before treatment to provide an electron density distribution. Mega Volt Cone Beam CT (MVCBCT) can be used for this purpose. A MVCBCT can be made while the patient is on the treatment couch. Portal images (PIs) are made from different angles from around the patient with an electronic portal imaging device (EPID) and are combined to yield a 3D image, that can be converted to electron density.

Due to scatter radiation reaching the EPID and beam hardening effects, the MVCBCT images experience cupping artifacts. If uncorrected, these cupping artifacts lead to errors in dose calculation. The focus of the present study is to correct the MVCB PIs of a phantom or patient for scattered radiation and beam hardening, without using prior knowledge of the geometry of the irradiated object.

Materials & Methods

A. Hardware and Operation

A Siemens Oncor linear accelerator with MV CB acquisition mode is used with an Optivue 1000 AG9 amorphous silicon EPID (Siemens Medical Solutions, Concord, USA).

Beam energy	6 MV
Field size (iso-plane)	27.4 x 27.4 cm
Dose rate	50 / 300 MU/min
Dose	2 to 60 MU
SDD	145 cm
EPID PIs	41 x 41 cm, 1024 x 1024 pixels
Reconstruction Volume	25.6^3 cm 256^3 voxels

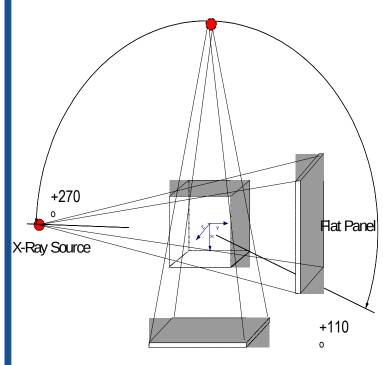

Figure 1: MVCBCT acquisition configuration.

During MV CB acquisition the gantry rotates continuously from +270° to +110° clockwise acquiring 200 projection images with increments of 1° (Figure 1).

The PIs are corrected for dead pixels and dark current. As well as for individual pixel sensitivities and the beam profile (gain images).

The reconstruction is performed with a research version of Cone Beam Reconstruction software provided by Siemens. A geometric calibration phantom is used to determine the relationship between the position of the voxels of the 3D image and the pixels of the EPID for each gantry angle.

B. Portal Image Correction

Before CB reconstruction we restored the beam profile and corrected for scatter radiation *S,* to yield the primary radiation *P*. *P* is corrected for the dependence of the attenuation coefficient μ_E, on the energy distribution of the incident photons. This is needed for the reconstruction software. The resulting signal is *P**, with

$$P^* \sim \exp(\mu \cdot t) \qquad (1)$$

and μ the attenuation coefficient for a mono-energetic photon-beam and *t* the radiological path length.

The incident beam profile is extracted from the gain image by assuming radial symmetry around the center pixel and calculating the mean of the gain image as function of the radial distance from the center (Figure 2).

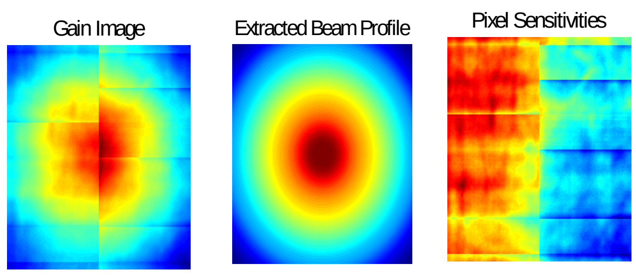

Figure 2: From left to right the raw gain image, the extracted beam profile and the pixel sensitivities

C.Scatter Prediction

The scatter distribution *S*, is estimated using the pencil beam concept, yielding

$$S(x,y) = \int_{x',y' \in Field} O(x',y') K(|x-x'|,|y-y'|, t_{(x',y')}, d) dx' dy' \qquad (2)$$

with *O* the open beam image, *x* and *y* the pixel coordinates and *d* the distances from the centers of mass of the object in the beam along the raylines to the detector. The kernel functions, *K*, are assumed to be Gaussian shaped and dependent on *t*, *r* and *d*. They are fitted with on-axis transmission measurements of slab phantoms of different *t* and with different field sizes.

D. Photon energy dependence correction

Large field PIs of slab phantoms of different *t* are made. The scatter transmission is calculated and extracted from the total measured transmission to yield the primary transmission $T^P(r,t)$, which relates $T^P(r)$ to *t* and through *t* to *P** (1).

E. Iterative PI correction model

The PI correction procedure requires a thickness map as input to calculate the scatter transmission. As our goal is to correct PIs without prior knowledge of the geometry of the object in the beam, a thickness map must be extracted from the CB PIs and open CB PIs. For this purpose an iterative PI correction model was designed (Figure 3). The convergence criterion is reached when

$$\frac{1}{N} \sum_{x,y} \left(t^{n+1}_{x,y} - t^{n}_{x,y} \right) < 0.05\,\text{cm} \qquad (3)$$

with *N* the number of pixels.

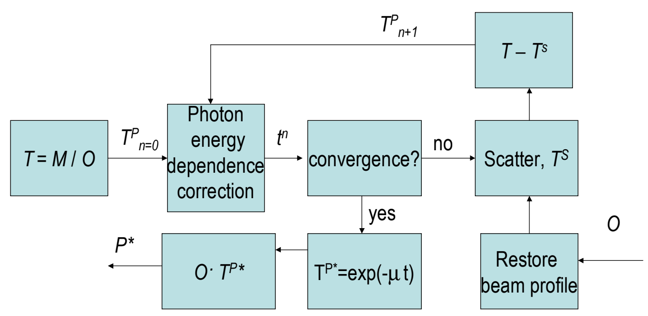

Figure 3: Iterative correction model, with T^P_n, T^S_n and t_n the n^{th} estimate of T^P, the scatter transmission T^S_n and *t* respectively, *O* the measured open beam and *M* the measured PI. The measured transmission *T*, is the first estimate of T^P.

F. Test Objects

MVCBCTs are made with 60 MU (50 MU/min) of a perspex cylinder filled with water (length = 30 cm, radius = 10 cm) and a brick phantom (14.2 x 14.5 x 29 cm) composed of polystyrene slabs.

Results

A comparison between the corrected and uncorrected MVCBCT images of the cylinder is shown in Figure 4. The cupping artifact is clearly visible in the uncorrected image but has disappeared in the corrected image. The error in the CT numbers of the voxels decreases from 11% to 3.4% (1 SD) .

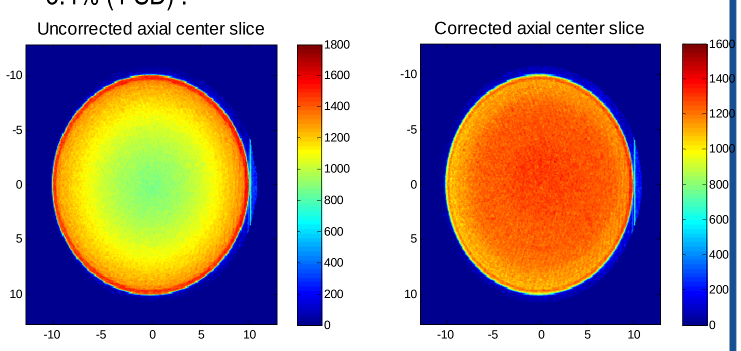

Figure 4: Left: CT-numbers of the central axial slice of the reconstructed image without correction. Right: CT-numbers of the center axial slice of the reconstructed image with correction. The used units are relative to electron density.

Histograms of the CT numbers of the voxels of the reconstructed images are shown in Figure 5. The corrected projections result in a smaller spread in electron density compared to the uncorrected projections. The standard deviations decrease from 120 (11%) to 43 (3.4%) and from 75 (6.4%) to 31 (2.4%) for the cylinder and the brick respectively.

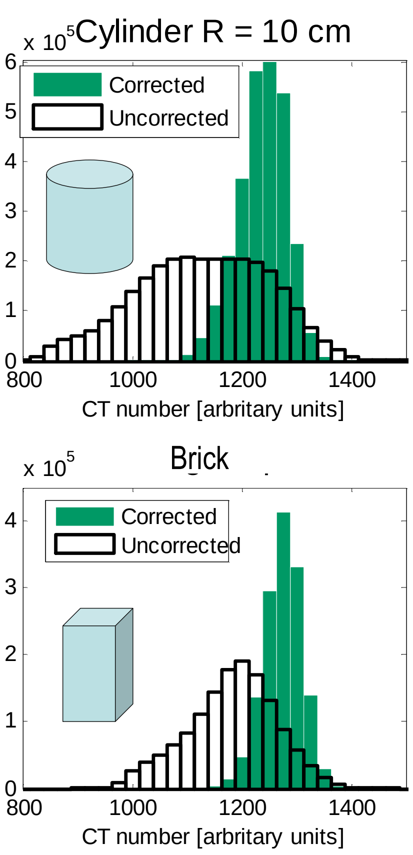

Figure 5: Histograms of the distribution of voxels as function of the reconstructed CT-number. The upper figure represents the cylinder and the bottom figure the brick.

Discussion / Conclusion

A model was designed capable of correcting cupping artifacts in MVCBCT images of arbitrary objects without using prior knowledge of the geometry. The model is accurate for the analyzed phantoms.

The iterative character of the correction scheme makes the model suitable for correcting PIs of patients, although the total dose is too high. Applying this model to low dose MVCBCT is promising.

The method experiences some difficulties in predicting electron density near the surface of the objects. The importance of these discrepancies must be evaluated with dose calculations. More research is being performed on correcting the PIs of other phantom geometries and on the calibration of the arbitrary CT-numbers to real electron density.

Acknowledgments

We would like to thank Siemens OCS for technical and financial support.

Correspondence to wouter.vanelmpt@maastro.nl

This poster can be found on www.maastro.nl/physics